Journal of Sol-Gel Science and Technology 38, 73–78, 2006

DOI: 10.1007/s10971-006-5035-0

Fabrication of Ordered TiO_2 Porous Thin Films by Sol-Dipping PS Template Method

ZHIFENG LIU, ZHENGGUO JIN*, XIAOXIN LIU, YANAN FU, AND GUOQI LIU
Key Laboratory for Advanced Ceramics and Machining Technology of Ministry of Education, School of Materials, Tianjin University, 300072, Tianjin, P. R. China
zhgjin@tju.edu.cn

Received August 18, 2005; Accepted September 15, 2005

Published online: 21 April 2006

Abstract. Monolayer polystyrene spheres (∼400 nm) array templates were assembled orderly on clean glass substrates by dip-drawing method from emulsion of PS and porous TiO_2 thin films were prepared by using sol-dipping template method to fill TiO_2 sol into the interstices among the close-packed PS templates and then annealing to remove the PS templates. The effects of TiO_2 precursor sol concentration and dipping time in sol on the porous structure of the thin films were studied. The results showed pore size of the ordered TiO_2 porous thin film depended mainly on PS size and partly on TiO_2 sol concentration. The shrinkage of pore diameter was about 10% for 0.2 M and 20% for 0.4 M TiO_2 sol concentrations. X-ray diffraction (XRD) spectra indicated the porous thin film was anatase structure. The transmittance spectrum showed that optical transmittance of the porous thin film kept above 70% beyond the wavelength of 430 nm. Optical band-gap of the porous TiO_2 thin film (fired at 550°C) was 3.12 eV.

Keywords: porous TiO_2 thin film, polystyrene spheres, sol-dipping template method, morphology

1. Introduction

TiO_2 semiconductor had a large direct band gap (3.2 eV), excellent chemical, thermal stability, and other physical properties. Porous nanocrystalline TiO_2 films had been attracted much attention because of their various applications in electronic, electrochemical, photoelectrochemical solar cells [1, 2], electrocatalysts [3], sensors [4], and high-performance photocatlysts [5]. For porous films including TiO_2, various chemical techniques had been employed, such as those based on selective etching [6], self-assembly of block copolymers [7], and close-packed colloidal crystal array templates [8–13]. The processing methods based on the close-packed array templates usually assemble close-packed arrays of monodispersed organic or inorganic spheres (typically polystyrene or silica) as templates by vertical deposition and gravity sedimentation method, and then fill the interstices among the close-packed arrays of polystyrene or silica spheres with a precursor, which forms a solid skeleton around the spheres. Finally, a well-defined porous material with narrow pore size distributions can be obtained when the templates are removed either by heat treatment or dissolution with a solvent.

In this paper, based on some previous works, we adopted a dip-drawing method both to assemble monolayer polystyrene spheres (PS) array templates and fill the interstices between PS array templates with TiO_2 sol. The assembly process of PS array template is described and the influences of TiO_2 sol concentration and dipping time in the TiO_2 sol on structural characteristics of the porous TiO_2 thin films are discussed. Also, phase composition and optical properties of the porous TiO_2 thin films are provided.

2. Experimental

2.1. Chemicals

In the preparation of PS and TiO_2 sol, the following materials were used: styrene (C_8H_8, AR), potassium persulfate ($K_2S_2O_8$, AR), 0.1 M sodium hydroxide, tetrabutylorthotitanate ($Ti(OC_4H_9)_4$, AR), diethanolamine

*To whom all correspondence should be addressed.

($NH(CH_2CH_2OH)_2$, AR), ethanol (CH_3CH_2OH, AR) and deionized water.

2.2. Synthesis

2.2.1. Synthesis of Monodispersed PS. Non-cross-linked, monodispersed PS were synthesized by using an emulsifier-free emulsion polymerization technique. Styrene (40 ml) was alternately washed in a separatory funnel four times with 50 ml of 0.1 M NaOH and 50 ml deionized water in order to remove polymerization inhibitor. A five-necked, 1000-ml round-bottomed flask was filled with 250 ml of water and 40 ml of the washed styrene and then heated to 70°C. Attached to the flask was an electric motor driving a glass string rod and Teflon wedge, a thermometer, a condenser, a pipe through which house nitrogen was bubbled to deaerate the mixture, and a stopper for the addition of reactants. In a separate bottle, small amount of potassium persulfate initiator was added to 50 ml of water, and heated to 70°C. Then the hot initiator solution was added drop-by-drop into the flask. The temperature was kept at 70 ± 2°C while the mixed solution was stirred at about 300 r/min for 15 h. The resulting latex spheres were remained suspended in their mother liquor until needed.

2.2.2. Assembly of the PS Array Templates. The PS array templates were assembled on clean glass substrates by a dip-drawing method. Firstly, Glass substrates (2 × 3 cm) were cleaned ultrasonically in acetone, 0.1 mol/L HCl solution, ethanol and deionized water, respectively. Then, the clean and dried glass substrate was settled vertically into the emulsion of PS for several minutes, and then slowly drew it out from the emulsion with a drawing rate of 0.1 cm/min and dried it in oven at 30°C for 15 min. The PS templates appeared opalescent, as expected, prismatic colors like rainbow, depending on the angle of observation, and clearly visible when the samples were illuminated from above with white light.

2.2.3. Synthesis of TiO_2 Sol. TiO_2 sol was prepared at room temperature in the following way: $Ti(OC_4H_9)_4$ was dissolved in the mixture solution of 35 ml ethanol and small amount of chelating agent ($NH(CH_2CH_2OH)_2$). The molar ratio of $NH(CH_2CH_2OH)_2$/$Ti(OC_4H_9)_4$ was 1:1. After magnetic stirring for 2 h, the obtained solution was hydrolyzed by the addition of a mixture of water and ethanol dropwise under stirring and then sequentially stirred for another 2 h.

2.2.4. Preparation of TiO_2 Thin Films. Sol-dipping template method was used to fill TiO_2 sol onto the PS templates. Firstly, the PS array templates on glass substrates were placed into different concentrations of TiO_2 sols (0.2–0.6 mol/L) and kept for 3 to 7 min. And then drawn out from the sol and dried in oven at 30°C for 1 h to form a solid skeleton around the spheres. At last, the poured templates were heated in air up to 550°C for 1 h at a heating rate of 2°C/min to remove the PS templates and obtain porous structure of TiO_2 thin films. Also, a dense TiO_2 thin film, as a reference sample, was prepared by the same sol-gel method using 0.4 M concentration and without PS templates. And the thickness of films could be adjusted by dipping cycle.

2.3. Characterization

TiO_2 sol viscosity was measured by using Ubbelohde Viscometer (Φ1.0, made in Shanghai China). Diameter of the PS was estimated by using transmission electron microscopy (TEM). Morphology of porous films was examined by using a PHILIPS XL-30 environment scanning electron microscopy (ESEM). X-ray diffraction (XRD) patterns of TiO_2 thin films were recorded with a Rigaku D/max-2500 using Cu Kα radiation ($\lambda = 0.154059$ nm). The optical transmittance of the films was detected by DU-8B UV/VIS double-beam spectrophotometer.

3. Results and Discussion

3.1. PS Array Templates

Figure 1 shows the TEM image of PS, which is synthesized by the emulsifier-free emulsion polymerization technique mentioned above. Its diameter is about 400 nm with a deviation of small than 5%.

Figure 2 shows the schematic of the dip-drawing method, which is used to assemble PS array templates. Its basic

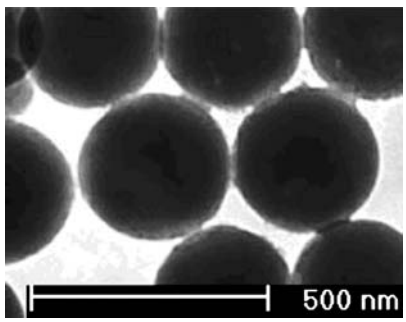

Figure 1. TEM image of polystyrene spheres.

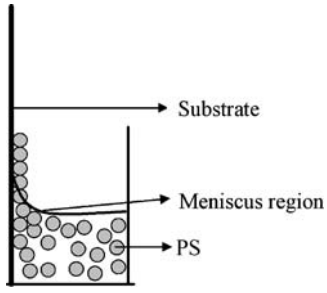

Figure 2. Schematic of assemble PS array template in PS emulsion.

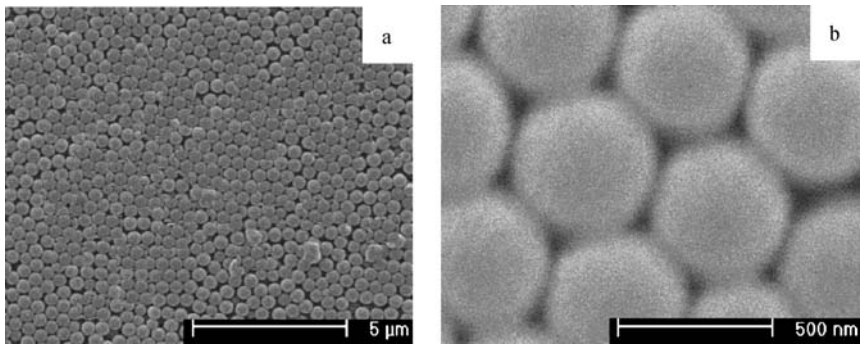

Figure 3. SEM images of PS templates (a) low-magnification; (b) high-maginification.

procedure is that a clean glass substrate is settled vertically into the emulsion of PS for several minutes, and then drew it up with a slower drawing rate. When the substrate was drawing out of the PS emulsion, a meniscus region on liquid surface near the substrate was formed due to wetting by the TiO_2 sol, which leads to the flux and accumulation of PS by means of interfacial tension. The template assembly process consists of PS accumulation at the intersectant place of air, PS emulsion and the substrate, transport of PS in the emulsion, and successive crystallization. In order to maximal decrease of PS template defects such as vacancies, dislocations, and plane stacking faults, the rate of nucleus formation, PS particles transport and crystallization should keep a balance during this process. Thus, the drawing rate of substrate plays an important role in the dip-drawing method. Higher drawing rate will lead to faster nucleus formation, lower PS transport time and smaller action time of capillary forces, as a result, there are not sufficient PS to explore favorite lattice sites of the PS template, leading to the formation of defects. However, there are some stacking faults on the intersectant place at over-slow drawing rate.

Figure 3 shows SEM images of the PS template made by the dip-drawing technique. From Fig. 3(a), the low-magnification image, we can see that the PS template has a highly ordered array on a lager area, but there are some defects at smaller local parts. Figure 3(b) is the high-magnification SEM image of the PS template, which shows the spheres are arranged in a close-packed fashion, with each sphere touching six others in one layer.

3.2. *Preparation of Porous TiO_2 Thin Films*

Figure 4(a) shows the preparation processing of porous TiO_2 thin films by the sol-dipping template method. The PS-covered glass substrate is settled vertically into the TiO_2 sol for several minutes. The precursor sol permeates the interstices of close-packed PS array template by capillary force. Then, the PS template imbued with TiO_2 sol is drawn out and the porous TiO_2 thin film can be obtained after removing the PS by heat treatment. It should be mentioned that the dip-drawing method has some advantages than that

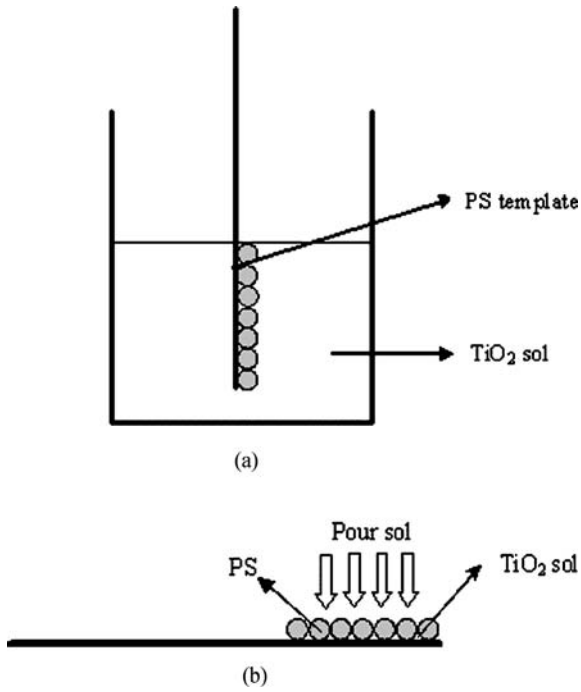

Figure 4. Schematic of sol-dipping template method (a) and vertical pour fashion (b).

showed in Fig. 4(b) [12, 13], i.e., the needed content of precursor to fill the PS interstices is difficult to control when the template is horizontal placed. If the content is more, the precursor will fully cover the top of PS template. Contrarily, precursor cannot fully pour the interstices of PS when the content is small. For the sol-dipping template method, the above disadvantage can be overcome by gravity due to vertical fashion.

3.3. *Morphology of Porous TiO_2 Thin Films*

Figure 5 shows the influence of sol concentration on the morphology of porous TiO_2 thin films (dipping time is 3 min). As showed in Fig. 5(a) and (b), the porous structure has been formed primarily but the inorganic wall is thin. This

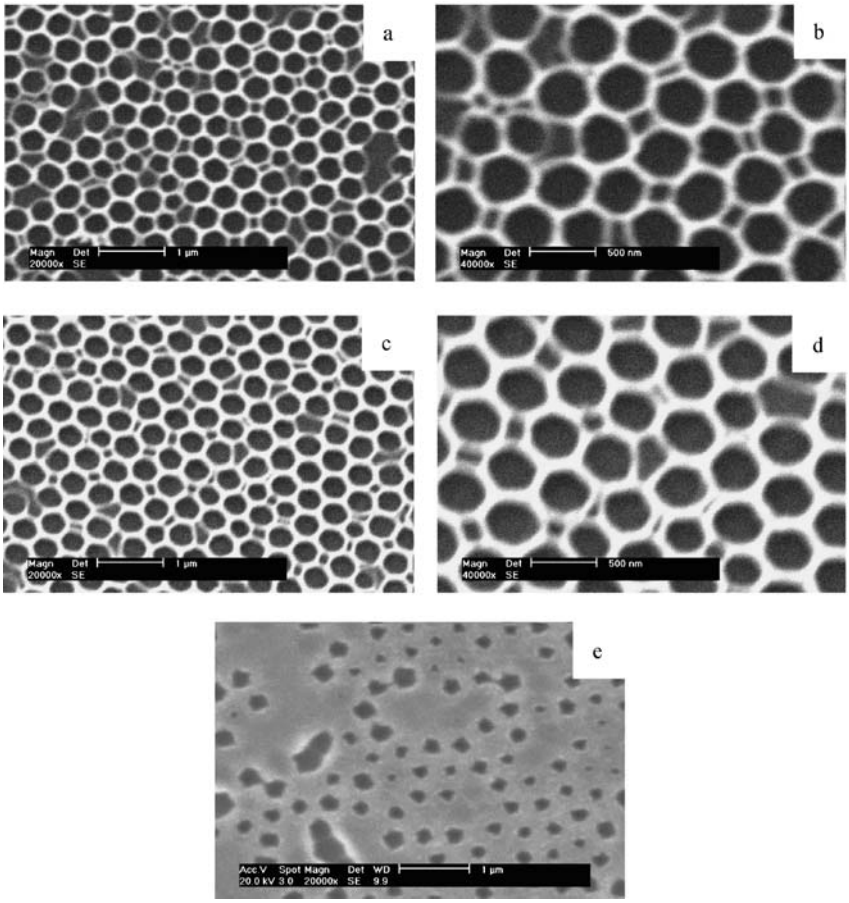

Figure 5. SEM images of TiO_2 thin films with different sol concentrations (a) (b) 0.2 M; (c) (d) 0.4 M; (e) 0.6 M.

indicates that the interstices are easy to be filled at lower concentration of TiO_2 sol (0.2 M) due to the lower viscosity (3.22cP), but there is no enough solid content when the template is removed. Figure 5(e) shows the morphology of thin film with the highest sol concentration (0.6 M) in our experiment. It can be seen that the porous structure cannot be formed after calcining because high concentration bring high viscosity (9.26cP), which results in a poor permeation among the close-packed arrays of PS. In conclusion, sol concentration plays an important role in the formation of ordered porous TiO_2 thin films. In this experiment the suitable sol concentration, which have a satisfactory permeation and a good pore structure, is about 0.4 M, and the corresponding viscosity is 5.81cP. From these images of the porous structure, it also can be seen that the ordered pores of TiO_2 thin film connect with each other by some small pores, which is caused by the less TiO_2 solid content, bigger fault interstices and the better affinity between TiO_2 sol and PS [14]. Moreover, it should be noted that the pore diameter depends on the size of PS used and the sol concentration. And typically, the average porous diameter of TiO_2 thin films is about 360 nm for 0.2 M sol concentration (Fig. 5(b)) and 320 nm for 0.4 M (Fig. 5(d)), corresponding to the pore shrinkage ratio is 10% and 20%, respectively. So, it could be understood that the decrease of pore size is due to the bulk shrinkage of PS during the volatilization, decompose and combustion of PS by annealing. At the same time, the solidification of TiO_2 gel in period of annealing enlarges the pore size of thin film. As a result, the final pore size is determined by the combination effect between the PS shrinkage and TiO_2 solidification. In addition, the thickness of porous TiO_2 thin films have been calculated from the top-view SEM images after removing PS templates. The film thickness of 0.2 M sol concentration and 0.4 M sol concentration is about 290 nm and 320 nm, respectively. Figure 6 shows the influence of dipping time in sol on the morphology of TiO_2 porous thin films (TiO_2 sol concentration is 0.4 M). It can be seen that the longer dipping time, the thicker porous wall, and the interconnected pores become smaller even disappear.

3.4. Characteristics of Porous TiO_2 Thin Films

Figure 7 shows X-ray diffraction (XRD) spectra of the TiO_2 thin films fired at temperature 550°C for 1 h. A dense TiO_2 film as contrast is also showed in Fig. 7. It should be noted that the thickness of dense film is similar to the porous one

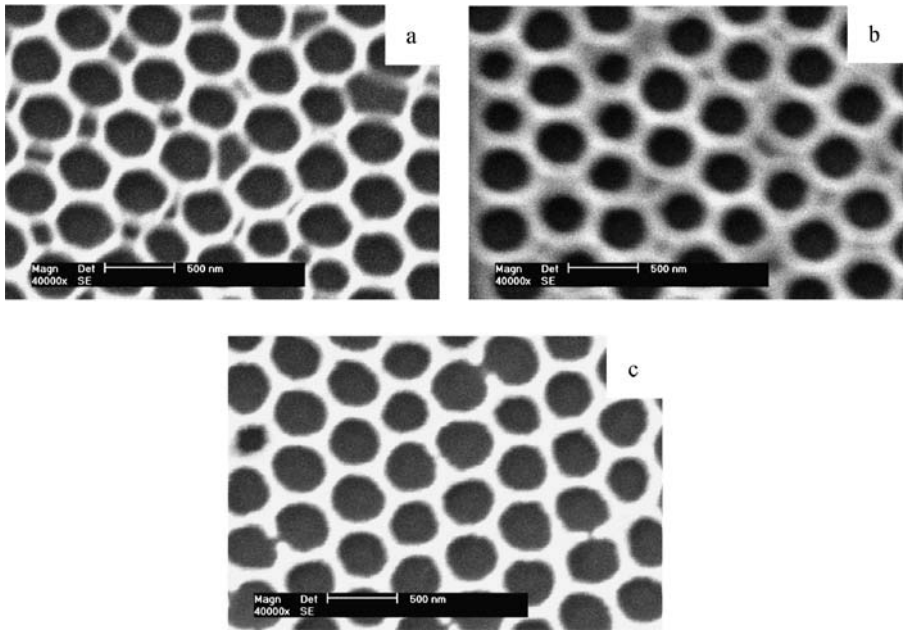

Figure 6. SEM images of TiO_2 thin films with different dipping time (a) 3 min; (b) 5 min; (c) 7 min.

made by sol-dipping PS template method. The bulge in the range of 15∼38° are the background diffraction of glass substrates. For the porous thin film, the peaks at $2\theta = 25.4°$ and 47.6° can be observed, corresponding to (101), (200) reflections of the anatase structure, respectively. These peaks can also be seen in the same positions for the dense sample. However, their peaks are stronger than those of the porous sample, indicating the negative effect of the porous structure on crystallization.

Figure 8 shows optical transmittance in the wavelength (λ) range 300∼800 nm for porous TiO_2 film, and a dense one with a similar thickness is also showed as a reference. From these, it can be seen that the optical transmittance of porous thin film decreases when compared with that of the dense one in the wavelength range of 350–800 nm, but still keep above 70% optical transmittances beyond the wavelength of 430 nm. This indicates that porous structure increase the interface scattering, which result in the decrease of transmission.

The absorption coefficient α is given by the transmittance T and film thickness d using the formula $\alpha = -\ln(T)/d$. The dependence of the absorption coefficient α upon the photon energy $h\nu$ for near edge optical absorption in semiconductors takes the form $\alpha h\nu = k(h\nu - E_g)^m$, Where E_g is the optical band gap, k is a constant and $m = 1/2$ for TiO_2 with an allowed direct energy gap. A typical $(\alpha h\nu)^2$ was plotted versus $h\nu$ using the data obtained from the optical absorption spectra (Fig. 9). The band gap of the as-prepared porous TiO_2 thin film is 3.12 eV, a slight decrease compared with the dense one (3.20 eV), which may be caused by the presence of defect level derived from the surface state of porous structure.

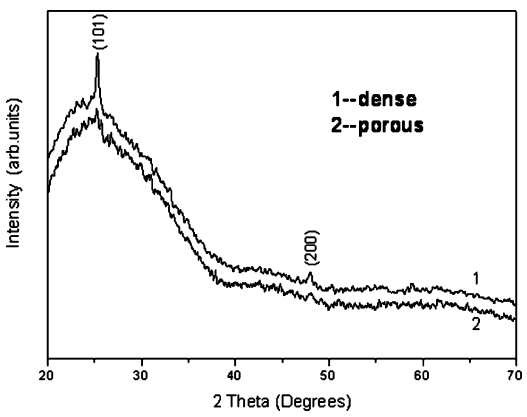

Figure 7. XRD patterns of TiO_2 films.

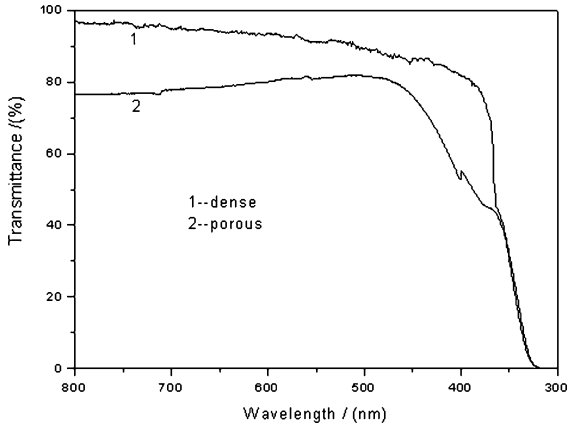

Figure 8. Optical transmittance spectra of TiO_2 films.

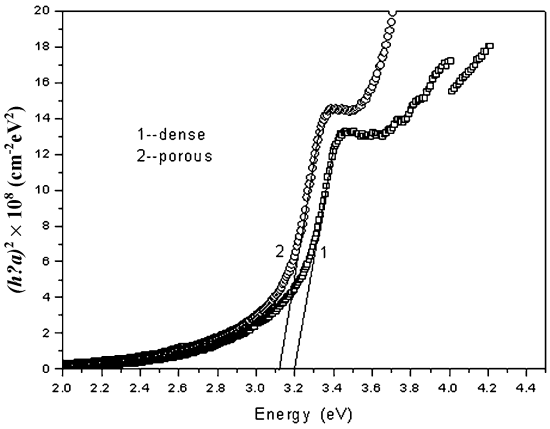

Figure 9. plot of $(\alpha h\nu)^2$ versus $h\nu$ for the TiO_2 films.

4. Conclusions

Polystyrene spheres (∼400 nm) were synthesized by an emulsifier-free emulsion polymerization technique and the monolayer PS array templates were assembled orderly on clean glass substrates by dip-drawing method from emulsion of PS. Porous TiO_2 thin films were prepared by using sol-dipping template method to fill TiO_2 sol into the interstices among the close-packed PS templates and then annealing to remove the PS templates. The results showed that TiO_2 precursor sol concentration and dipping time played important roles on the formation of porous morphology. An ordered TiO_2 porous thin film with the designed pore size that partly depended on the sol concentration could be obtained. And the shrinkage between the pore diameter of TiO_2 thin films and PS was about 10–20%. The thin films were anatase structure observed by X-ray diffraction (XRD) spectra. The transmittance spectrum showed that optical transmittance of the porous thin film decreases when compared with that of the dense one in the wavelength range of 350–800 nm, but still kept above 70% beyond the wavelength of 430 nm. Optical band-gap of the porous TiO_2 thin film (fired at 550°C) was 3.12 eV.

Acknowledgments

The authors (Z. G. Jin, Z. F. Liu) gratefully acknowledge financial support from Natural Science Foundation of Tianjin (No. 033802311).

References

1. B. O'Regan and M. Grätzel, Nature **353**, 737 (1991).
2. B. O'Regan, D.T. Schwartz, S.M. Zakeeruddin, and M. Grätzel, Adv. Mater. **12**, 1263 (2000).
3. B.B. Lakshmi, P.K. Dorhourt, and C.R. Martin, Chem. Mater. **9**, 857 (1997).
4. H.M. Lin, T.Y. Hsu, C.Y. Tung, and C.M. Hus, Nanostructured Mater. **6**, 1001 (1995).
5. K.R. Gopidas, M. Bohorques, and P.V. Kamat, J. Phys. Chem. **94**, 6435 (1990).
6. R.C. Furneaux, W.R. Rigby, and A.P. Davidson, Nature **337**, 147 (1989).
7. G. Widawski, M. Rawiso, and B. Francois, Nature **369**, 387 (1994).
8. L.I. Halaoui, N.M. Abrams, and T.E. Mallouk, J. Phys. Chem. B **109**, 6334 (2005).
9. P.N. Bartlett, J.J. Baumberg, P.R. Birkin, M.A. Ghanem, and M.C. Netti, Chem. Mater. **14**, 2199 (2002).
10. H. Yan, C.F. Blanford, B.T. Holland, W.H. Smyrl, and A. Stein, Chem. Mater. **12**, 1134 (2000).
11. G. Subramanian, V.N. Manoharan, J.D. Thorne, and D.J. Pine, Adv. Mater. **11**, 1261 (1999).
12. Y. Shen, Q. Wu, J. Liao, and Y. Li, J. Inorg. Mater. **18**, 401 (2003).
13. Y. Shen, Z. Sun, and Y. Li, J. Inorg. Mater. **19**, 939 (2004).
14. Y. Shen, Q. Wu, and Y. Li, Acta Scientiarum Anturalium Universitatis Sunyatseni (China), **41**, 45 (2002).